Follicle Detection Model on Ovarian Ultrasound_Image.pdf

By Angga Pradipta

WORD COUNT	5219	TIME SUBMITTED	20-NOV-2023 09:07AM
		PAPER ID	104372275

Follicle Detection Model on Ovarian Ultrasound Image

Sri Hartati
Department of Computer Science and Electronics
Universitas Gadjah Mada
Yogyakarta, Indonesia
shartati@ugm.ac.id

Aina Musdholifah
Department of Computer Science and Electronics
Universitas Gadjah Mada
Yogyakarta, Indonesia
aina_m@ugm.ac.id

Putu Desiana Wulaning Ayu
Department of Information Technology, Faculty Computer and Informatics Institut Teknologi dan Bisnis STIKOM Bali
Bali, Indonesia
wulaning_ayu@stikom-bali.ac.id

Jaswadi Dasuki
Faculty of Medicine, Public Health and Nursing
Universitas Gadjah Mada
Yogyakarta, Indonesia
djaswadi@ugm.ac.id

2022 Seventh International Conference on Informatics and Computing (ICIC) | 979-8-3503-4571-1/22/$31.00 ©2022 IEEE | DOI: 10.1109/ICIC56845.2022.10006915

***Abstract*— every woman has two ovaries. Ovaries have several follicles, which consist of oocytes or eggs which are filled with granulosa cells. Some women can have a difference in the number of follicles in each ovary. There are cases of several follicles that are coincided, making it difficult to calculate the number of follicles. In this study, the separation of adjoining follicles and automatic follicle counting was carried out from the results of ovarian ultrasound image segmentation. The segmentation results obtained feature information in the form of follicular feature extraction as many as eight features. The techniques used in this work for feature selection was carried out using Principal Components Analysis (PCA) to reduce the feature. In this study, the PCA and Support Vector Machine (SVM) classifier produced higher accuracy than the classification without PCA. The experimental results also show that the proposed method produced higher classification accuracy than previous work, which yielded 90.39% accuracy, 90.27 % sensitivity, and 90.43 % specificity.**

Keywords— Follicle, Principal Components Analysis, Support Vector Machine.

I. Introduction

Follicular monitoring is essential for diagnosing, treating, and preventing infertility [1]. Infertility in women of reproductive age can be experienced by patients diagnosed with Polycystic Ovary Syndrome (PCOS). PCOS is a reproductive and metabolic disorder. PCOS can affect 6% - 20% of women of childbearing age worldwide, with a prevalence reaching or even exceed 10–15% [2]–[7]. PCOS patients have many follicles and a small follicle size [8], [9]. European Society for Human Reproduction and Embryology (ESHRE) and the American Society for Reproductive Medicine (ASRM) described polycystic ovary as having 12 or more follicles 2-9 mm in size, and ovarian volume are greater than 10 cm^3. The polycystic ovary can be seen from the results of an ultrasound image. Normal ovarian morphology when less than 12 follicles <10 mm of diameter or dominant follicle (> 10mm) were counted in follicular number per section [3], [4], [10]. Sample images of normal ovarian morphology [4] and polycystic ovarian morphology [3], as shown in Fig. 1. There are two ways of ultrasound examination, namely transabdominal and transvaginal ultrasound. Polycystic ovary is seen more clearly using transvaginal ultrasound examination [11]–[14]. Transvaginal ultrasound examination was performed by gynecologists in the early follicular phase of menstruation and independently of the cycle phase in amenorrhea patients [15].

Transvaginal ultrasound is often used to examine ovarian conditions because it is safe, and the results of the images can be printed immediately. It also used to provide consultation to patients to monitor the growth of ovarian follicles [16]. Follicle monitoring based on ultrasonographic images takes time to count small follicles [16]. Computer-aided diagnostic techniques have been used for ovarian monitoring, follicle segmentation to better understand the condition of the ovarian follicles. There are still few studies on applying computer-aided diagnostic techniques to detect follicles from ultrasound images of ovaries automatically. Research for follicle detection on ovarian ultrasound images using thresholding [17], active contour [18], watershed [19], region growing [20]-[21], horizontal window filtering and filled Convex hull technique [22], automatic follicle segmentation using the k-means clustering method was successful [23]. However, the resulting follicle segmentation was still unable to separate adjoining follicles, which affected the count of follicles. The contribution of this research are some cases follicles are coincided, this will make it difficult to calculate the number of follicles. This study carried out the separation of adjoining follicles and automatic follicle counting from the results of ovarian ultrasound image segmentation using Active Contour Without Edge and Watershed modification. The results of segmentation get a variety of feature extraction values, then the most relevant feature will be selected using feature selection.

Computer-aided diagnostic techniques have been used for ovarian monitoring, follicle segmentation to better understand the condition of the ovarian follicles. There are still few studies on applying computer-aided diagnostic techniques to detect follicles from ultrasound images of ovaries automatically. Research for follicle detection on ovarian ultrasound images using thresholding [17], active contour [18], watershed [19], region growing [20]-[21], horizontal window filtering and filled Convex hull technique [22], automatic follicle segmentation using the k-means clustering method was successful [23]. However, the resulting follicle segmentation was still unable to separate

adjoining follicles, which affected the count of follicles. The novelty of this research are some cases follicles are coincided, this will make it difficult to calculate the number of follicles. This study carried out the separation of adjoining follicles and automatic follicle counting from the results of ovarian ultrasound image segmentation using Active Contour Without Edge and Watershed modification. The results of segmentation get a variety of feature extraction values, then the most relevant feature will be selected using feature selection.

Fig. 1. Sample images of ovarian morphology [3] [4]

II. Related Work

Several approaches have proposed to segmentation the follicle from an ultrasound image of the ovary. Some researchers in follicle testing used preprocessing, segmentation, feature extraction and classification stages. The preprocessing stage is done with median filtering, adaptive median filtering, gaussian filtering and contourlet transform.

Optimal thresholding segmentation using for automated detection of the follicle in the ultrasound image, Sobel operator and morphological gap and shutting is used for preprocessing. Feature extraction is predicated on seven geometric parameters of the follicles [17]. The segmentation method is implemented using active contour without edge and watershed for automated detection of the follicle in the ultrasound image of the ovary. Feature extractions used are area, perimeter, centroid, roundness [18].

In [19], they use edge-based segmentation and morphological operations to detect 50 sample images. The preprocessing stage for noise reduction is implemented using a Gaussian low pass filter or contourlet transform for despeckling the ultrasound images of ovaries. Geometric features used are major axis length, minor axis length, the ratio of major axis length to minor axis length.

Region growing segmentation resulted in follicle recognition of about 78% but difficulty detecting smaller follicles due to their brightness in the dataset [20]. Research [21] with the region growing method resulted in follicle recognition higher than [19], but this method is limited to ultrasound images with homogeneity [21]. Ardhendu Mandal, Manas Sarkar, and Debosmita Saha [22] used morphological opening followed by morphological closing operations for speckle noise ultrasound image of the ovary. Horizontal Window Filter (HWF), filled convex hull technique and active contours for follicle segmentation from ovarian USG image, the success rate of follicle detection is 94.03% in classification and 87.23% in precision [22]. Follicle segmentation from ovarian ultrasound image using active contour yields high accuracy for large and small follicles, but the segmentation is not automatic [18]. Segmentation using the k-means clustering method [23] succeeded in recognizing follicles automatically, but follicles that were attached follicles were still not recognized properly.

In [25], they are used a cost map depending on the pixel's relative location and region growing method for follicle identification with recognition rate for all the images processed is 84.04% and misidentification rate is 5.9%. In [26], they applied a morphological operation with an edge-based method using a canny operator for follicle identification and an average recognition rate of 87.5%. In this paper used active contour without edge and watershed modification for segmented the follicles, especialy separation of adjoining follicles and automatic follicle counting.

III. Proposed Method

The framework of the proposed method for automatic follicle detection is shown in Fig. 2. This article primarily divides the segmentation algorithm into six steps: image acquisition, preprocessing, segmentation, feature extraction, feature selection, and classification.

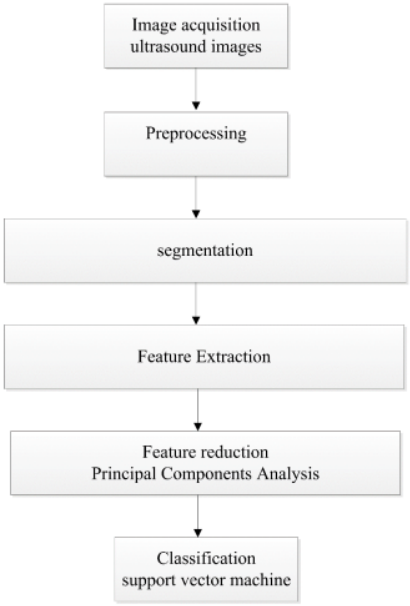

Fig. 2. The proposed method for automatic follicle detection

A. Image acquisition and preprocessing

Image acquisition is the process of taking follicle image from ultrasound images of the ovaries. In this study, we use the data from the Sakina Idaman General Hospital Yogyakarta. For this research used 90 image ulatrasound. The initial step for the preprocessing is determine the region of interest, change the original image to the grayscale image, histogram equalization, and speckle noise reduction the ultrasound images of the ovaries used adaptive median filtering.

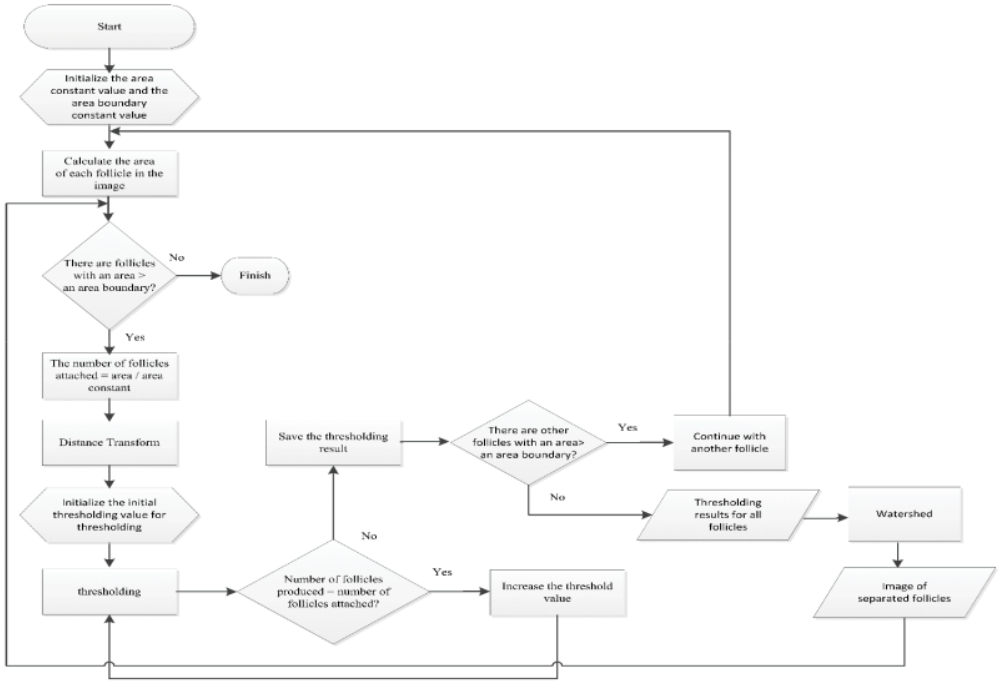

Fig. 3. Automatic detection of coincided follicles

B. Segmentation Process

The segmentation process produces sub-images that contain the only follicle. The segmentation is done using binarization, morphological operations, hole filling operations, active contour without edge and watershed modification for automatic follicle detection is shown in Fig. 3.

C. Equations Feature Extraction

Segmentation produces an image object that will be used for the feature extraction stage. The object in this study is the follicles. This research will use feature extraction in the form of geometric shape features. Geometric shape features such as area, perimeter, major axis, minor axis, eccentricity, extent, circularity, and tortuosity are measured to identify the correct follicle.

X_1 : Area
X_2 : Perimeter
X_3 : Major Axis
X_4 : Minor Axis
X_5 : Eccentricity
X_6 : Extent
X_7 : Circularity
X_8 : Tortuosity

The bounding box area is a basic descriptive property. It is easy to calculate the area from the curve boundary representations and the chain code [27]. The perimeter is the length of the object's edge or outline [28]. The object area is known as the white area expressed by the number of pixels of the selected object area [28], [29]. An area with all interior corners less than 180^0 is the area convex used to determine the type of object [30]. The ratio of the area to the area of the bounding box will give the extents [28]. Formula for extent show in equation (1).

$$Extent = \frac{object\ area}{boundingbox\ area} \quad (1)$$

Area and convex area have a relationship to characterize the form solidity of the object [30]. The relationship between area and perimeter can produce circularity, which is the roundness of the object [30]. Eccentricity is the distance between the centre of an ellipse and the length of its major axis. The range of the value is between 0 and 1[27]. The ellipse has 2 focal points called foci. Comparison of the distance between the foci and the major axis will produce eccentricity [28], [30]. The length of the major axis is the scalar that determines the length in pixels of the major axis of the ellipse, having the same normalized second centre momentum as the region [29]. The minor axis length is a scalar that defines the length in pixels of an ellipse's minor axis having the same normalized second centre momentum as the region. The axis ratio is the ratio between the length of the major axis and the length of the minor axis [30]. Tortuosity is defined as the ratio of the length of the major axis to the perimeter. Compactness is a measure of conciseness, not conciseness in terms of point-collection topology, which has no dimensions and is minimized by a disk.

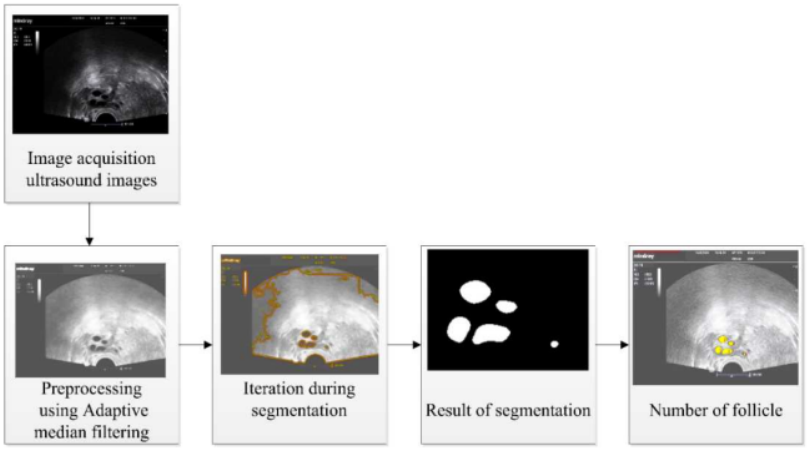

Fig. 4. Image of the automatic follicle detection

$$= 4\pi\left(\frac{Circularity}{\frac{Area}{perimeter^2}}\right) \quad (2)$$

$$Eccentricity = \frac{Distance\ between\ ellipse\ Foci}{Length\ of\ Major\ axis} \quad (3)$$

$$Tortuosity = \frac{major\ axis}{perimeter} \quad (4)$$

D. Feature Selection

Feature selection is a method to reduce the features that will be used for classification, hoping that the results will increase accuracy, reduce computation time, and eliminate features that are less relevant [31]. The feature selection method is effective if it can produce as few features as possible but can produce high accuracy. In this study, Principal Component Analysis (PCA) is implemented to reduce the feature. Then the accuracy results are compared with the accuracy of the classification results without PCA. PCA provide as much information as possible in the data using the least-squares approach. PCA reduces the dimensions of the data by retaining as much information as possible from the original dataset. The stages of image processing using PCA are calculating the average value of the image, representing it in the form of mean corrected data, calculating covariance matrices, finding eigenvalues and eigenvectors, and performing reductions.

PCA projects the data along a direction where the data has high variance. The direction is determined by the eigenvectors of the covariance matrix, which have the largest eigenvalues. The value of the eigenvalues is the variance value of the data along the direction of the eigenvector. Steps for feature selection using PCA [32] :

1. Find the mean (average value) of the data

Suppose $x_1, x_2, \ldots, x_M$ are contained in the vector N x 1

$$\bar{x} = \frac{x_1 + x_2 + \cdots + x_M}{M} = \frac{\sum_{i=1}^{M} x_i}{M} \quad (5)$$

2. Calculating Zero Mean for each value in the sample data minus the average value of each associated feature.

$$\Phi_i = x_i - \bar{x} \quad (6)$$

3. Construct a Covariance matrix by multiplying the Zero Mean matrix with the transposition of the Sample Population

$$C = \frac{1}{M}\sum_{i=1}^{M} \Phi_i^T \Phi_i \quad (7)$$

$$C = \frac{1}{M-1}\sum_{i=1}^{M} \Phi_i^T \Phi_i \quad (8)$$

4. Calculate the eigenvalue of C. Result $\lambda_1, \lambda_2, \lambda_3, \ldots \ldots \ldots \lambda_N$

$$CU = \lambda U$$
$$ICU = I\lambda U$$
$$CU = \Lambda iu$$
$$(\lambda I - C)U = 0$$
$$det(\lambda I - C) = 0 \quad (9)$$

5. Calculating the eigenvector matrix, from the eigenvalue calculated in step 4, is substituted into the formula:

$$(\lambda I - C)U = 0 \quad (10)$$

Finish by finding a value U

Result $u_1, u_2, u_3, \ldots \ldots \ldots u_N$

E. Classification Method

The classification uses the Support Vector Machine (SVM), looking for the best hyperplane as a separator of the two classes in the input space. The best separator hyperplane between the two classes can be found by measuring the hyperplane's margin and finding its maximum point. Margin

is the distance between the hyperplane and the closest pattern from each class [33]. SVM can classify data that are linearly separable and nonlinear separable. Some of the kernel commonly used in the SVM method is Linear, Polynomial, Radial basis function (RBF) and Sigmoid using kernel parameters. SVM kernels that are often used, namely linear, polynomial and radial basis functions, the radial basis function kernel is the best accuracy level [33], [34].

1. Linier : $\mathrm{K}(x_i, x_j) = x_i^T x_j$ (11)
2. Polynomial: $\mathrm{K}(x_i, x_j) = \left(\gamma x_i^T x_j + r\right)^d, \gamma > 0$ (12)
3. *Radial basis function (RBF)*:
   $\mathrm{K}(x_i, x_j) = \exp\left(-\gamma \left\| x_i - x_j \right\|^2\right), \gamma > 0$ (13)
4. Sigmoid: $\mathrm{K}(x_i, x_j) = \tanh(\gamma \cdot x_i^T + r)$ (14)

IV. RESULT AND DISCUSSION

In the proposed method, there are 4 stages to extract each follicle. First is image acquisition, pre-processing using adaptive median filtering, segmentation using active contour without edge and watershed, and feature extraction for each follicle. Fig. 4 shown the image of automatic follicle detection.

PCA is an analysis technique for transforming original attributes correlated with one another into a new and uncorrelated set of attributes. Each follicle that has been segmented produces feature values $(X_1, X_2, X_3 \ldots X_8)$, representing data according to the selected dataset.

TABLE 1. FEATURE EXTRACTION DATA

No.	X_1	X_2	X_3	X_4	X_5	X_6	X_7	X_8
1	456	98.6274	35.2099	17.3692	0.8698	0.6096	0.5890	0.3570
2	568	96.9705	28.1372	26.0341	0.3793	0.6802	0.7590	0.2901
3	488	97.5563	31.3651	20.7250	0.7505	0.6931	0.6443	0.3215
4	388	84.9705	27.4279	18.6401	0.7335	0.6461	0.6753	0.3227
5	300	70.7279	21.3370	18.4725	0.5005	0.6575	0.7536	0.3016
6	460	90.6274	28.4949	21.0829	0.6727	0.6969	0.7037	0.3144
7	436	100.3848	39.0420	15.1509	0.9216	0.6728	0.5437	0.3889
8	526	94.3259	36.3597	18.9801	0.8529	0.5903	0.7429	0.3854
9	507	101.7401	37.4562	19.6206	0.8518	0.5451	0.6155	0.3681
10	256	64.6274	21.8529	15.5748	0.7014	0.6485	0.7702	0.3381
11	528	97.8406	32.7006	21.3394	0.7577	0.6173	0.6931	0.3342
⋮	⋮	⋮	⋮	⋮	⋮	⋮	⋮	⋮
281	594	97.5978	29.7733	26.2157	0.4740	0.7394	0.7831	0.3050

TABLE 2. MEAN AND STANDARD DEVIATION FOR DATASET FEATURE EXTRACTION

	X_1	X_2	X_3	X_4	X_6	X_7	X_8	X_9
Mean	1129.238	138.381	42.048	27.114	0.728	0.620	0.619	0.323
standard deviation	1711.342	99.443	25.669	17.258	0.137	0.081	0.171	0.047

TABLE 3. STANDARDIZE THE DATASET FOR EACH FEATURE

No.	X_1	X_2	X_3	X_4	X_5	X_6	X_7	X_8
1	0.209053	0.961195	0.884244	0.270295	1.046244	-0.47787	-1.62331	-0.99525
2	0.178668	0.750735	0.408011	0.818325	-0.79058	-1.22656	-1.2975	-1.64064
3	1.188986	1.540399	1.655936	1.319061	0.581021	-0.19106	-0.88511	-0.71102
4	-0.0241	0.837073	0.094223	0.59389	-1.35352	-0.56727	-1.993	-2.62156
5	-0.08487	0.311477	0.13551	0.279566	-0.11025	-0.63059	-1.09803	-1.16408
6	0.516414	0.54104	0.584426	1.058921	-0.88902	0.755033	0.384214	-0.56569
7	0.156463	0.374253	0.264723	0.706892	-0.97944	0.490572	-0.29198	-0.96533
8	-0.15499	0.196696	0.131922	0.010148	0.523415	-0.64301	-1.07405	-0.76231
9	0.457981	0.627378	0.60087	0.988542	-0.64256	-0.04456	-0.13346	-0.79222
10	6.708632	3.81852	4.717183	4.164034	0.489872	0.388761	-0.16856	-0.18102
11	-0.30692	-0.30753	-0.25219	-0.23484	0.245594	0.669362	0.200542	0.143815
⋮	⋮	⋮	⋮	⋮	⋮	⋮	⋮	⋮
281	-0.31276	-0.41011	-0.47821	-0.05206	-1.8501	1.480126	0.960969	-0.39045

Table 1 is the features set from each follicle. There is 281 image of follicles. Each follicle has 8 features, including area, perimeter, major axis, minor axis, eccentricity, extent, circularity, and tortuosity. The dataset has a striking difference in scale between features. This scale difference can cause asymmetry of data distribution, so it is necessary to standardize the dataset. Standardization of the dataset is carried out after obtaining the whole data's mean and standard deviation value. Table 2 displays the results of the mean and standard deviation for each feature. Table 3 shows the results of the data standardization process that will be used to calculate the covariance matrix.

The next stage is calculate the covariance matrix for the whole dataset. Covariance is implemented to measure the size of the relationship between two dimensions. If the covariance is calculated from one dimension with the dimension itself, the result is the variance. In a similar way, we calculate the other covariances, and the result is in Table 4. The next step is to calculate the eigenvalue and eigenvector of the covariance matrix. The eigenvalues and eigenvectors contain useful information from a dataset. They are also used to determine the principal component (PC) involved. Table 5 shows the results of the eigenvector values.

The feature vector Table 6 shows the eigenvalues, variability and cumulative values for PC1, PC2, PC3, PC4, PC5, PC6, PC7 and PC8. PC1 represent 55.34% of the total data, PC2 represent 80.44% of the total data, PC4 represent 97.91% of the total data, and PC8 represent 100% of the total data. Support Vector Machine algorithm using the Radial Basis Function (RBF) kernel is implemented as a classifier. First, the dataset is divided into training data and testing data. It was carried out using k-fold 10 on the whole dataset.

SVM was used as a classifier for big follicle and small follicle. Evaluation of model performance is applied using several statistical parameters, namely accuracy, sensitivity, and specificity. Accuracy is a measure to see the level of success of the classification carried out. Sensitivity is the classifier's ability to predict a positive class as positive (true positive), while specificity is the classifier's ability to recognize a negative class as negative (true negative).

TABLE 4. COVARIANCE MATRIX FOR THE WHOLE DATASET

	X_1	X_2	X_3	X_4	X_6	X_7	X_8
X_1	1	0.9087	0.9159	0.9081	-0.0283	0.0078	-0.3030
X_2	0.9087	1	0.9694	0.9441	0.0112	-0.1477	-0.5680
X_3	0.9159	0.9694	1	0.9189	0.1292	-0.1541	-0.5166
X_4	0.9081	0.9441	0.9189	1	-0.2080	0.0193	-0.3808
X_5	-0.0283	0.0112	0.1292	-0.2080	1	-0.4907	-0.3284
X_6	0.0078	-0.1477	-0.1541	0.0193	-0.4907	1	0.6559
X_7	-0.3030	-0.5680	-0.5166	-0.3808	-0.3284	0.6559	1
X_8	-0.3905	-0.5820	-0.4270	-0.6111	0.5521	-0.0518	0.4744

TABLE 5. EIGENVECTOR

	PC1	PC2	PC3	PC4	PC5	PC6	PC7	PC8
PC1	-0.4264	-0.0809	-0.3422	-0.2025	-0.6409	-0.4647	-0.1102	-0.1210
PC2	-0.4700	0.0086	-0.0914	0.0469	0.1438	-0.0101	0.3456	0.7926
PC3	-0.4534	0.0590	-0.2425	0.0252	0.2307	0.2778	0.5282	-0.5676
PC4	-0.4521	-0.1557	-0.1114	-0.1499	0.3382	0.2987	-0.7299	-0.0097
PC5	0.0219	0.6113	-0.3861	0.4775	0.2689	-0.3642	-0.2072	-0.0296
PC6	0.0850	-0.5928	-0.3095	0.7032	-0.1546	0.1609	-0.0294	0.0224
PC7	0.2910	-0.4109	-0.4459	-0.3755	0.4840	-0.3993	0.1134	0.0054
PC8	0.3080	0.2678	-0.5997	-0.2650	-0.2656	0.5473	-0.0035	0.1829

TABLE 6. PRINCIPAL COMPONENT RESULTS ON VARIANCE DATASET FOR FOLLICLE FEATURE EXTRACTION

	PC1	PC2	PC3	PC4	PC5	PC6	PC7	PC8
Eigenvalue	4.427	2.007	1.083	1.034	0.068	0.063	0.023	0.012
Variability (%)	55.34	25.10	13.55	3.93	0.85	0.79	0.29	0.16
Cumulative (%)	55.34	80.44	93.98	97.91	98.76	99.55	99.84	100

TABLE 7. EVALUATION OF MODEL PERFORMANCE USING SVM

	Non-PCA	PC1	PC2	PC3	PC4	PC5
Accuracy	89.68%	90.04%	90.04%	90.04%	**90.39%**	89.68%
Specificity	89.30%	89.78%	89.78%	89.78%	**90.27%**	89.30%
Sensitivity	90.43%	90.53%	90.53%	90.53%	**90.63%**	90.43%

$$\text{Accuracy} = \frac{TP + TN}{TP + TN + FP + FN} \quad (15)$$

$$\text{Specifity} = \frac{TN}{TN + FP} \quad (16)$$

$$\text{Sensitivity} = \frac{TP}{TP + FN} \quad (17)$$

The evaluation results of the various features used can be seen in Table 7. When using 5 PC, the accuracy is the same as when without using PCA. In this study, the best accuracy was obtained when using 4 PC.

The previous research method [20] used region growing segmentation, resulting in follicle recognition, and the accuracy is 89.4% from 31 ultrasound images of ovaries . Other methods that use active contour for follicle segmentation directly from 15 ultrasound images of ovaries have 81.03% in accuracy and 87.23% in precision [22]. In [25], the region growing method is implemented for follicle identification with a recognition rate is 84.04% and a misidentification rate is 5.9%. In [26], the edge-based method using a canny operator is implemented for follicle identification from 12 ultrasound images of ovaries, and the average recognition rate is 87.5%. 15 ultrasound images of ovaries have 81.03% in accuracy and 87.23% in precision [22]. In [25], the region growing method is implemented for follicle identification with a recognition rate is 84.04% and a misidentification rate is 5.9%. In [26], the edge-based method using a canny operator is implemented for follicle identification from 12 ultrasound images of ovaries, and the average recognition rate is 87.5%. The accuracy of the proposed method is 90.39%. Meanwhile, the sensitivity is 90.27%, and the specificity is 90.43%.

V. Conclusion

The proposed method aims to identify ovarian morphology using ultrasound images. Ovarian morphology shows the number of follicles in the ovaries. In this research, PCA is used to improve accuracy when classification. The most relevant features are 4 features. The results of SVM classification using the PCA feature have an accuracy of 90.39%, 90.27 % sensitivity, and 90.43 % specificity. The results obtained were able to show that the proposed methods were able to identify ovarian morphology. The method proposed in this study can be considered one part of developing a computer-aided design to determine the condition of ovarian follicles. In future work, it is suggested to propose other classification technique for follicle detection.

Acknowledgment

This research was supported by Rekognisi Tugas Akhir (RTA) program from the Research Directorate of Universitas Gadjah Mada through contract number 3190/UN1/DITLIT/DIT-LIT/PT/2021.

References

[1] E. A. Ford, E. L. Beckett, S. D. Roman, E. A. McLaughlin, dan J. M. Sutherland, "Advances in human primordial follicle activation and premature ovarian insufficiency," *Reproduction*, vol. 159, no. 1, hal. R15–R29, Jan 2020.

[2] N. E. H. Mimouni, I. Paiva, A.-L. Barbotin, F. E. Timzoura, D. Plassard, S. Le Gras, G. Ternier, P. Pigny, S. Catteau-Jonard, V. Simon, V. Prevot, A.-L. Boutillier, dan P. Giacobini, "Polycystic ovary syndrome is transmitted via a transgenerational epigenetic process," *Cell Metab.*, vol. 33, no. 3, hal. 513–530.e8, Mar 2021.

[3] T. T. Lee dan M. E. Rausch, "Polycystic Ovarian Syndrome: Role of Imaging in Diagnosis," *RadioGraphics*, vol. 32, no. 6, hal. 1643–1657, Okt 2012.

[4] D. Chizen and R. Pierson, "Transvaginal ultrasonography and female infertility," *Glob. Libr. women's Med.*, 2010.

[5] Rotterdam ESHRE/ASRM-Sponsored PCOS Consensus Workshop Group, "Revised 2003 consensus on diagnostic criteria and long-term health risks related to polycystic ovary syndrome," *Fertil. Steril.*, vol. 81, no. 1, hal. 19–25, Jan 2004.

[6] I. Kyrou, M. O. Weickert, dan H. S. Randeva, "Diagnosis and Management of Polycystic Ovary Syndrome (PCOS)," in *Endocrinology and Diabetes*, London: Springer London, 2015, hal. 99–113.

[7] M. L. and I. P. N. Teede HJ, Misso ML, Costello MF, Dokras A, Laven J, "Recommendations from the international evidence-based guideline for the assessment and management of polycystic ovary syndrome†‡," *Hum. Reprod.*, vol. 33, no. 9, hal. 1602–1618, Sep 2018.

[8] S. G. Kristensen, A. Kumar, B. Kalra, S. E. Pors, J. A. Bøtkjær, L. S. Mamsen, L. B. Colmorn, J. Fedder, E. Ernst, L. A. Owens, K. Hardy, S. Franks, dan C. Y. Andersen, "Quantitative Differences in TGF-β Family Members Measured in Small Antral Follicle Fluids From Women With or Without PCO," *J. Clin. Endocrinol. Metab.*, vol. 104, no. 12, hal. 6371–6384, Des 2019.

[9] S. Agrawal, "Polycystic Ovary Syndrome," in *Endocrine Conditions in Pediatrics*, Cham: Springer International Publishing, 2021, hal. 267–270.

[10] A. M. Fulghesu, E. Canu, L. Casula, F. Melis, dan A. Gambineri, "Polycystic Ovarian Morphology in Normocyclic Non-Hyperandrogenic Adolescents," *J. Pediatr. Adolesc. Gynecol.*, Feb 2021.

[11] G. S. Conway, J. W. Honour, dan H. S. Jacobs, "Heterogeneity Of The Polycystic Ovary Syndrome: Clinical, Endocrine And Ultrasound Features In 556 Patients," *Clin. Endocrinol. (Oxf).*, vol. 30, no. 4, hal. 459–470, Apr 1989.

[12] S. R. Goldstein, "Incorporating endovaginal ultrasonography into the overall gynecologic examination," *Am. J. Obstet. Gynecol.*, vol. 162, no. 3, hal. 625–632, Mar 1990.

[13] A. H. Balen, J. S. E. Laven, S. Tan, dan D. Dewailly, "Ultrasound assessment of the polycystic ovary : international consensus de ® nitions," vol. 9, no. 6, hal. 505–514, 2003.

[14] T. Bourne, L. Hamberger, M. Hahlin, dan S. Granberg, "Ultrasound in gynecology: endometrium.," *Int. J. Gynaecol. Obstet.*, vol. 56, no. 2, hal. 115–127, 1997.

[15] A. La Marca dan S. K. Sunkara, "Individualization of controlled ovarian stimulation in IVF using ovarian reserve markers: from theory to practice," *Hum. Reprod. Update*, vol. 20, no. 1, hal. 124–140, Jan 2014.

[16] W. P. Martins and L. Jokubkiene, "Assessment of the functional ovarian reserve in Managing Ultrasonography in Human Reproduction: A Practical Handbook," *Springer, pp. 3-12, 2017*, no. Cham, Switzerland.

[17] Hiremath P. S. and Tegnoor J. R., "Automatic Detection of Follicles in Ultrasound Images of Ovaries by Optimal Threshoding Method," *Int. J. Comput. Sci. Inf. Technol.*, vol. 3(2) 217-2, 2010.

[18] Eliyani, S. Hartati, dan A. Musdholifah, "Machine Learning Assisted Medical Diagnosis for Segmentation of Follicle in Ovary Ultrasound," 2019, hal. 71–80.

[19] Eliyani, S. Hartati, A. Musdholifah, dan D. Dasuki, "Active Contour Without Edge and Watershed for Follicle Detection in Ultrasound Image of Ovary," in *2020 International Conference on Advanced Computer Science and Information Systems (ICACSIS)*, 2020, hal. 295–300.

[20] Y. Deng, Y. Wang, dan Y. Shen, "An automated diagnostic system of polycystic ovary syndrome based on object growing," *Artif. Intell. Med.*, vol. 51, no. 3, hal. 199–209, 2011.

[21] B. Potočnik dan D. Zazula, "Automated ovarian follicle segmentation using region growing," *Int. Symp. Image Signal Process. Anal. ISPA*, vol. 2000–Janua, no. February, hal. 157–162, 2000.

[22] A. Mandal, M. Sarkar, dan D. Saha, "Follicle Segmentation from Ovarian USG Image Using Horizontal Window Filtering and Filled Convex Hull Technique," 2021, hal. 555–563.

[23] V. Kiruthika dan M. M. Ramya, "Automatic Segmentation of Ovarian Follicle Using K-Means Clustering," *2014 Fifth Int. Conf. Signal Image Process.*, hal. 137–141, 2014.

[24] U. M. Khaire dan R. Dhanalakshmi, "Stability of feature selection algorithm: A review," *J. King Saud Univ. - Comput. Inf. Sci.*, Jun 2019.

[25] R. Sitheswaran dan S. Malarkhodi, "An effective automated system in follicle identification for Polycystic Ovary Syndrome using ultrasound images," *2014 Int. Conf. Electron. Commun. Syst. ICECS 2014*, 2014.

[26] B. Padmapriya dan T. Kesavamurthy, "Detection of follicles in poly cystic ovarian syndrome in ultrasound images using morphological operations," *J. Med. Imaging Heal. Informatics*, vol. 6, no. 1, hal. 240–243, 2016.

[27] D. H. Ballard dan C. M. Brown, *Computer Vision*. New Jersey (US): Prentice Hall., 1982.

[28] B. Wenger, S. Mandayam, P. J. Violante, dan K. J. Drake, "Detection of anomalous events in shipboard video using moving object segmentation and tracking," *AUTOTESTCON (Proceedings)*, hal. 261–266, 2010.

[29] R. C. . Gonzalez dan R. E. Woods, "Digital image processing," *Nueva Jersey*. hal. 976, 2008.

[30] Z. Chen dan T. Ellis, "Multi-shape descriptor vehicle classification for urban traffic," *Proc. - 2011 Int. Conf. Digit. Image Comput. Tech. Appl. DICTA 2011*, hal. 456–461, 2011.

[31] T.-K. Lin, "PCA/SVM-Based Method for Pattern Detection in a Multisensor System," *Math. Probl. Eng.*, vol. 2018, hal. 1–11, 2018.

[32] S. Wold, K. Esbensen, dan P. Geladi, "Principal component analysis," *Chemom. Intell. Lab. Syst.*, vol. 2, no. 1–3, hal. 37–52, Agu 1987.

[33] C. Cortes dan V. Vapnik, "Supprot-Vector Networks," *Mach. Learn.*, vol. 297, no. 20, hal. 273–297, 1995.

[34] E. A. Borovikov, "An Evaluation of Support Vector Machines as a Pattern Recognition Tool," *Learning*, 1999.

[35] Vapnik V., *Statistical Learning Theory*. John Wiley, 1998.

Follicle Detection Model on Ovarian Ultrasound_Image.pdf

ORIGINALITY REPORT

11%
SIMILARITY INDEX

PRIMARY SOURCES

1	www.semanticscholar.org Internet	107 words — 2%
2	library.iugaza.edu.ps Internet	79 words — 2%
3	rain.atmos.colostate.edu Internet	76 words — 2%
4	"Proceedings of International Conference on Frontiers in Computing and Systems", Springer Science and Business Media LLC, 2021 Crossref	74 words — 2%
5	res.mdpi.com Internet	72 words — 2%
6	Tirta Farisaldi Ibrahim, Setiawardhana, Riyanto Sigit. "Support Vector Machine: Melanoma Skin Cancer Diagnosis based on Dermoscopy Image", 2022 International Electronics Symposium (IES), 2022 Crossref	67 words — 2%

EXCLUDE QUOTES	ON	EXCLUDE SOURCES	< 2%
EXCLUDE BIBLIOGRAPHY	ON	EXCLUDE MATCHES	OFF